

Supporting Information

Aggregation-Induced Phosphorescence of an Anthraquinone Based Emitter

Goudappagouda,^{a,b} Aakash Nidhankar,^{a,b} Rashmi A. Nayak,^a Sukumaran Santhosh Babu^{*a,b}

a. Organic Chemistry Division, National Chemical Laboratory (CSIR-NCL), Dr. Homi Bhabha Road, Pune-411008, India.

b. Academy of Scientific and Innovative Research (AcSIR), New Delhi-110020, India.

Content

1. Experimental	Page S2
2. Synthesis	Page S4
3. Figures S1 to S25	Page S8
4. Tables S1- S10	Page S26
5. References	Page S34

Experimental

Materials

All chemicals, 2,6-Diaminoanthraquinone, hexanoyl chloride were purchased from commercial suppliers and used as such without further purification. Solvents such as N,N-dimethylformamide (DMF) were purified prior to use according to the standard protocol and stored in molecular sieves.

Thin-layer chromatography was carried out using Aluchrosep Silica Gel 60/UV₂₅₄ purchased from Merck Specialties Pvt. Ltd.

All the reactions were carried out in oven-dried round bottom flasks under argon atmosphere unless otherwise mentioned.

General

The ¹H, ¹³C NMR spectra were recorded at Bruker-400 MHz NMR spectrometer instrument. The chemical shift values for ¹H (TMS as internal standard) and ¹³C NMR are recorded in CDCl₃. The value of coupling constant (*J*) is stated in Hertz (Hz). MALDI-TOF MS spectrum was recorded using DHB (2,5-dihydroxybenzoic acid) as the inert matrix on AB SCIEX MALDI TOF/TOFTM 5800. UV-Vis absorption spectra were recorded with a Shimadzu 1800 spectrophotometer, while all emission spectra were performed using PTI Quanta Master™ Steady State Spectrofluorometer. Fluorescence lifetimes were measured by time-correlated single photon counting (TCSPC), using a spectrofluorometer (Horiba scientific) and LED excitation source is 374 nm. The quality of the fit has been judged by fitting parameters such as χ^2 (<1.2) as well as visual inspection of the residuals. Phosphorescence spectra were recorded using Fluorolog-3 HORIBA JOBIN VYON spectrophotometer. Phosphorescence lifetime using decay by delay method was measured on a Horiba QM400 fluorescence spectrometer. Absolute luminescence quantum yield was measured using a Quanta-Phi 6" model F-3029. Single crystal X-ray intensity data was collected on a Bruker SMART APEX II CCD diffractometer with graphite-monochromatized (Mo K α = 0.71073 Å) radiation at ambient temperature.

Details of DFT calculations

Ground (S₀) state calculations were performed using restricted density functional theory (DFT). Singlet and triplet excited states were investigated using time-dependent density functional theory (TDDFT).^{S1} The ground state singlet (S₀) state was calculated using B3LYP/6-31G(d)^{S2} level of theory. Also the TDDFT calculations were done with same level of theory. All the geometries of the complexes in the S₀ state were optimized. The optimized Cartesian coordinates and total energies are listed below. On the basis of the Frank-Condon principle, the absorption properties were evaluated using the optimized S₀ state structure. The Gaussian09 software^{S3} was used in all the DFT and TDDFT calculations.

Phosphorescence Experiments

All phosphorescence experiments were measured at room temperature (298 K) in air by keeping the same experimental parameters. The window of maximum delay after flash for phosphorescence measurements was kept as 3 ms for -196 °C and 0.3 ms for 298 K. The wavelength of excitation is $\lambda_{ex} = 374$ nm. Phosphorescence lifetimes were measured at room temperature (298 K) in air by keeping 10% delay component and 10% trigger pulse duration, using 415 nm excitation source.

Single crystals

A single crystal of **AqC6** was grown in DMF. Single crystal X-Ray analysis and the same samples were used for all the characterization and optical measurements to get consistent results. Single crystal structure analysis shows that crystals of **AqC6** (CCDC 2050268) belong to the Monoclinic P2₁/c (14) space group.

Preparation of AqC6 PMMA film.^{S4}

Firstly, prepared a different weight percent of PMMA in CHCl₃ (95 %, 70 %, 50 %, 30 %, 20 %, 10 % and 5 %) and 100 μL of this solution is added to 100 μL of a solution of **AqC6** in DMF having different weight percent (5 %, 30 %, 50 %, 70 %, 80 %, 90 % and 95 %). The use of chloroform improves morphology and gives more glassy nature to the film. 100 μL of this solution was drop-casting onto the cleaned quartz substrates, and kept for solvent evaporation on hot plate at 80 °C for 10 min.

Calculation of photophysical parameters

The photophysical parameters were calculated using the following equations.

$$k_r^{Phos} = \phi_{Phos} / \tau_{Phos}$$

$$k_{nr}^{Phos} = (1 - \phi_{Phos}) / \tau_{Phos}$$

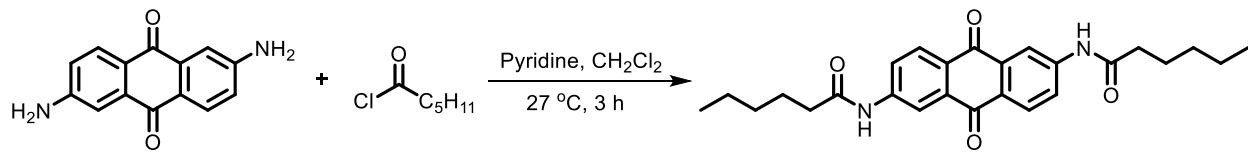
Where,

ϕ_{Phos} : Phosphorescence quantum yield

τ_{Fluo} : Fluorescence lifetime

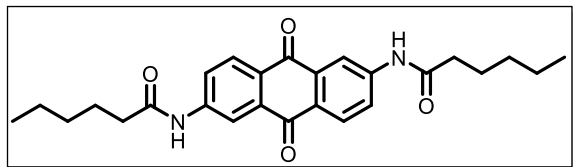
τ_{Phos} : Phosphorescence lifetime

Synthesis



Scheme S1. Synthesis of N,N'-(9,10-dioxo-9,10-dihydroanthracene-2,6-diyl)diheptanamide (AqC6).^{S5}

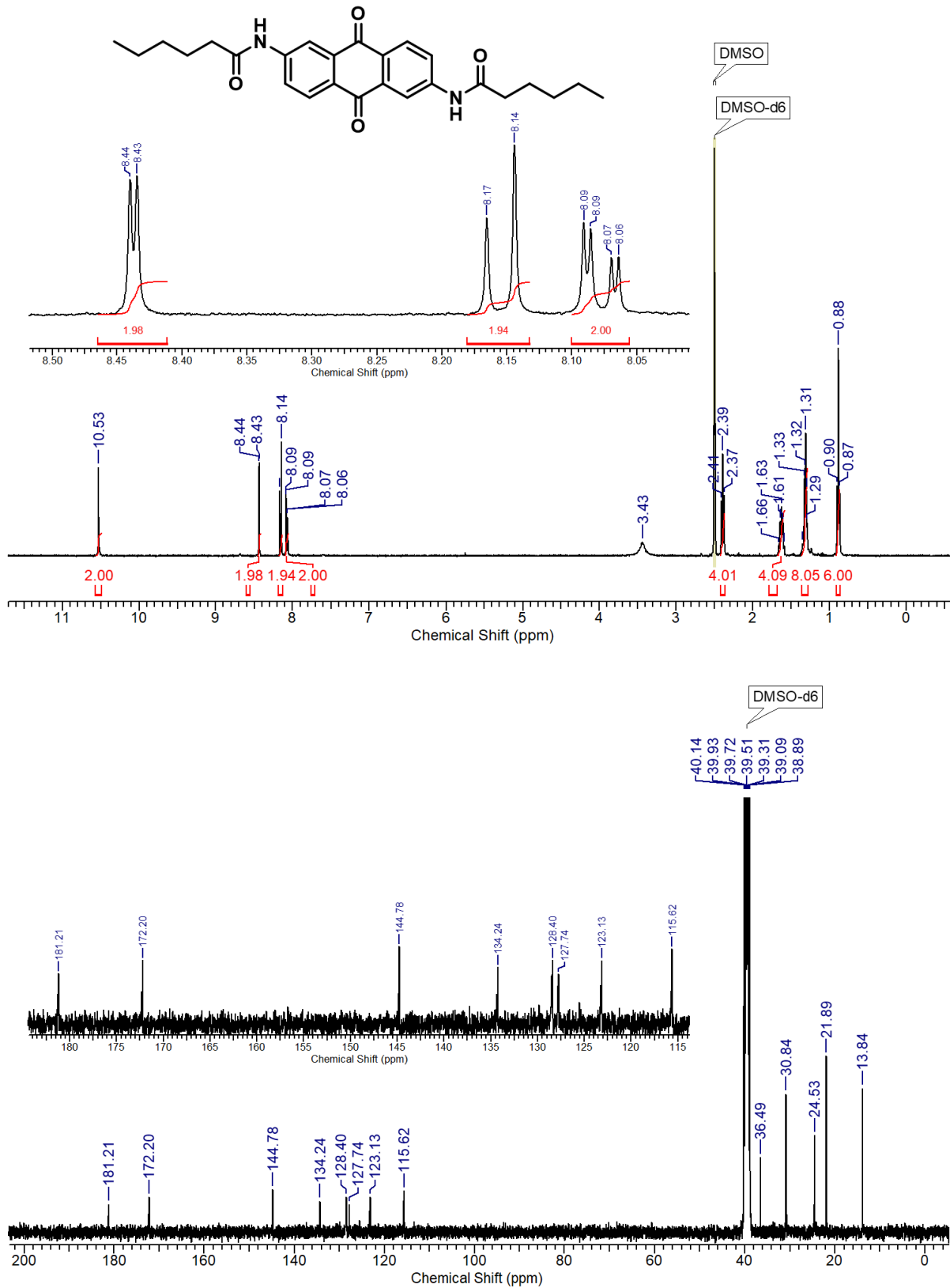
2,6-Diaminoantraquinone (1.0 g, 4.2 mmol), pyridine (4.5 mL, 50.33 mmol) were taken in an RB flask with dichloromethane (10 mL). Hexanoyl chloride (2.93 mL, 20.99 mmol) was added to the reaction mixture in drop-wise, and the resulting mixture was stirred at 27 °C for 3 h, during which the color changed from red to yellow. The resulting mixture was filtered and washed with 1 M HCl, and then washed with diethyl ether. The yellow solid was digested in refluxing ether for 1 h, then filtered again, giving the title compound (1.7 g, 93 %) as a yellow powder.



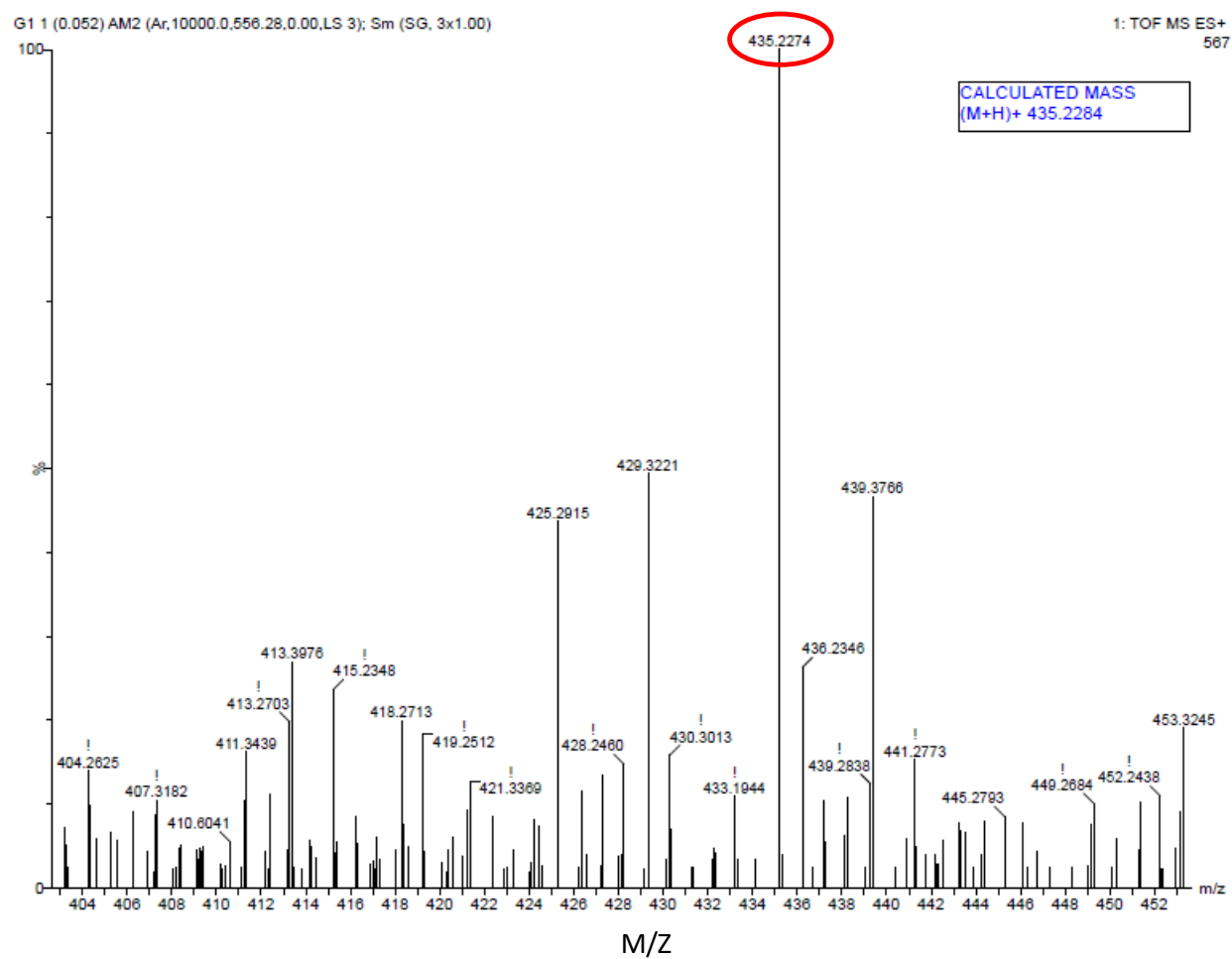
¹H NMR (400 MHz, DMSO-d6), δ (TMS, ppm): 10.53 (s, 2H), 8.44 (d, J = 2.13 Hz, 2H), 8.13-8.18 (m, 2H), 8.08 (dd, J = 2.19, 8.57 Hz, 2H), 2.39 (t, J = 7.44 Hz, 4H), 1.63 (quin, J = 7.32 Hz, 4H), 1.28 -1.35 (m, 8H), 0.86 -0.91 (t, 6H).

¹³C NMR (101 MHz, DMSO-d6), δ (TMS, ppm): 181.2, 172.2, 144.8, 134.2, 128.4, 127.7, 123.1, 115.6, 36.5, 30.8, 24.5, 21.9, 13.8

HR-MS (ESI⁺): calcd for $\text{C}_{26}\text{H}_{30}\text{N}_2\text{O}_4$ [M+H]⁺ 434.2284, found 434.2274.



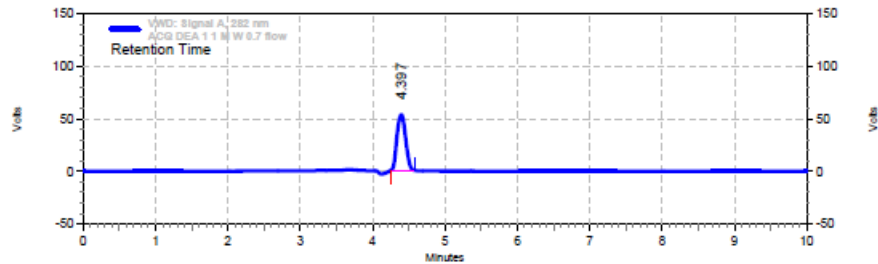
¹H (top) and ¹³C (bottom) NMR spectra of *N,N'*-(9,10-dioxo-9,10-dihydroanthracene-2,6-diyl)diheptanamide (**AqC6**).



HR-MS spectra of *N,N'*-(9,10-dioxo-9,10-dihydroanthracene-2,6-diyl)dihexanamide (**AqC6**).

Area % Report

Data File: E:\Year 2021\Jan 2021\4.1.2021 (Ruxo std)\ACQ DEA 1 1 M W 0.7 flow.rslt\ACQ DEA 1 1 M
 W 0.7 flow.dat
 Method: C:\Enterprise\Method\007.met
 Acquired: 04-01-2021 17:20:03 (GMT +05:30)
 Printed: 04-01-2021 18:38:39 (GMT +05:30)



VWD: Signal A,
 282 nm Results

<u>Retention Time</u>	<u>Area</u>	<u>Area %</u>	<u>Height</u>	<u>Height %</u>
4.397	7426282	100.00	888051	100.00
Totals	7426282	100.00	888051	100.00

Sample id: - ACQ

Mode: - RP-LC

Port: - D Pump

Flow rate: - 0.7 mL/min

Composition: - MeOH: H₂O:DEA (70:30:0.1)

Column: - ShimPak (250mm * 4.6mm * 5uM)

HPLC profile of **AqC6** (RT = 4.397), in MeOH:H₂O:DEA (70:30:0.1) mixture by monitoring at 282 nm.

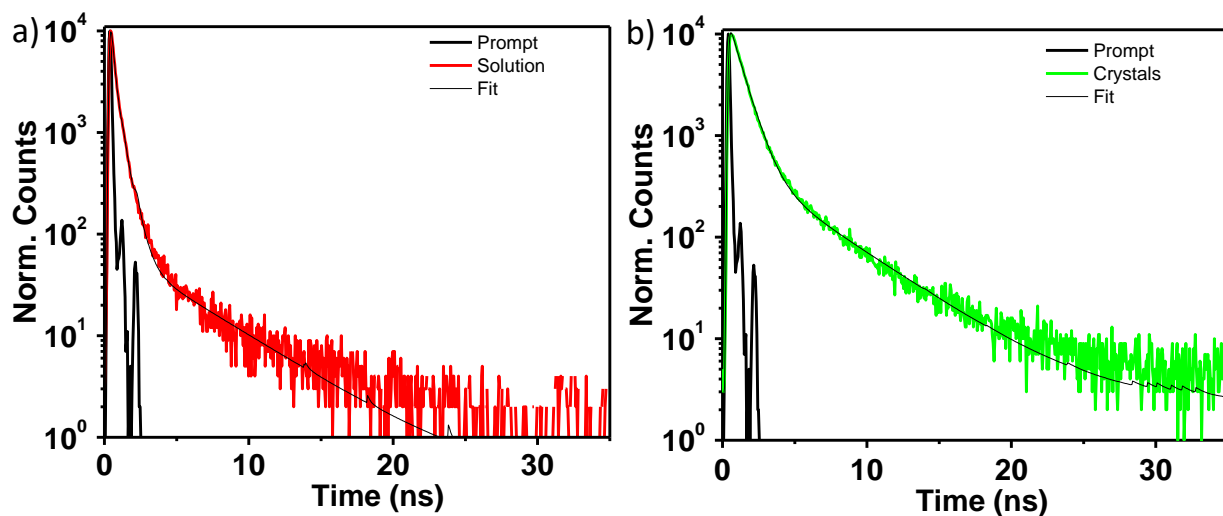


Figure S1. Emission lifetime decay profile of **AqC6** a) solution in DMF ($C = 1 \times 10^{-5}$ M, $l = 1$ cm, $\lambda_{\text{ex}} = 374$ nm, $\lambda_{\text{mon}} = 410$ nm), b) crystals ($\lambda_{\text{ex}} = 374$ nm, $\lambda_{\text{mon}} = 560$ nm).

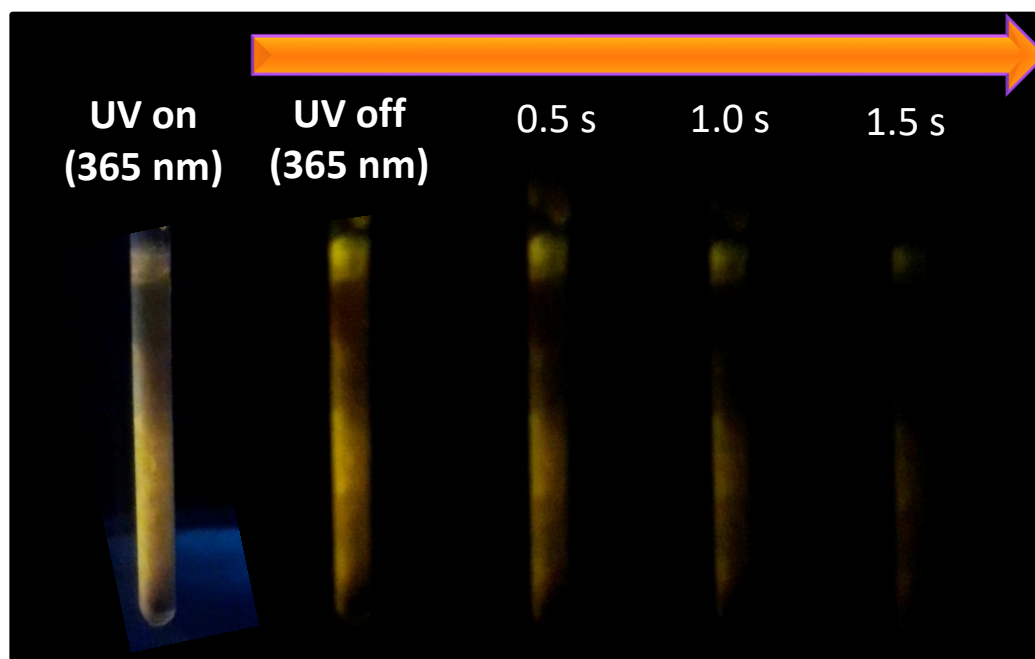


Figure S2. Phosphorescence images of **AqC6** DMF solution in a quartz tube (3 mm) recorded at different time intervals upon turning off the excitation source (365 nm) after 3 s exposure at 77 K.

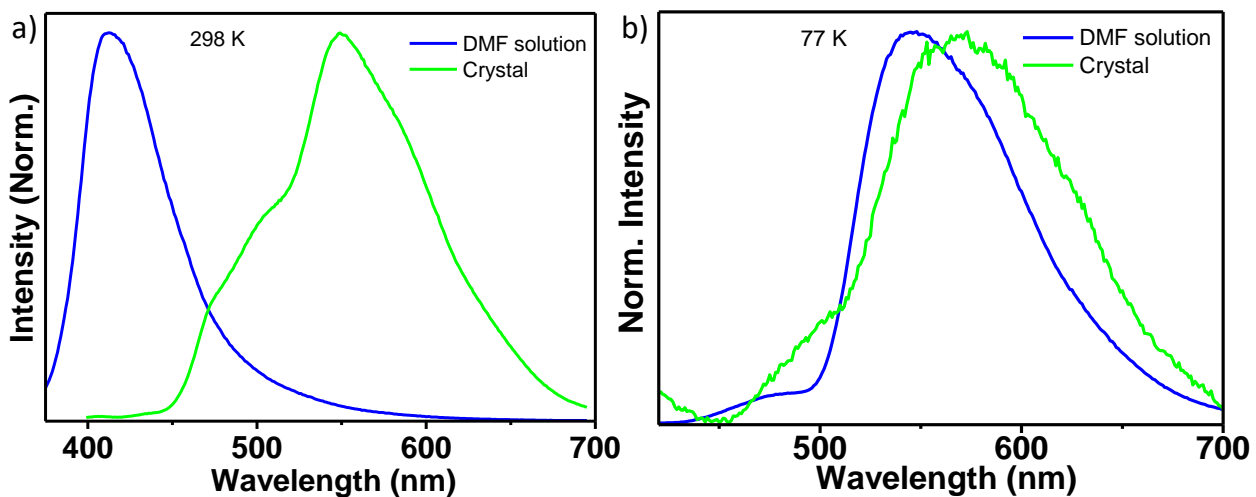


Figure S3. Comparison of the normalized steady-state emission of **AqC6** in DMF solution and crystal state ($\lambda_{\text{ex}} = 374 \text{ nm}$) at a) 298 K and b) 77 K.

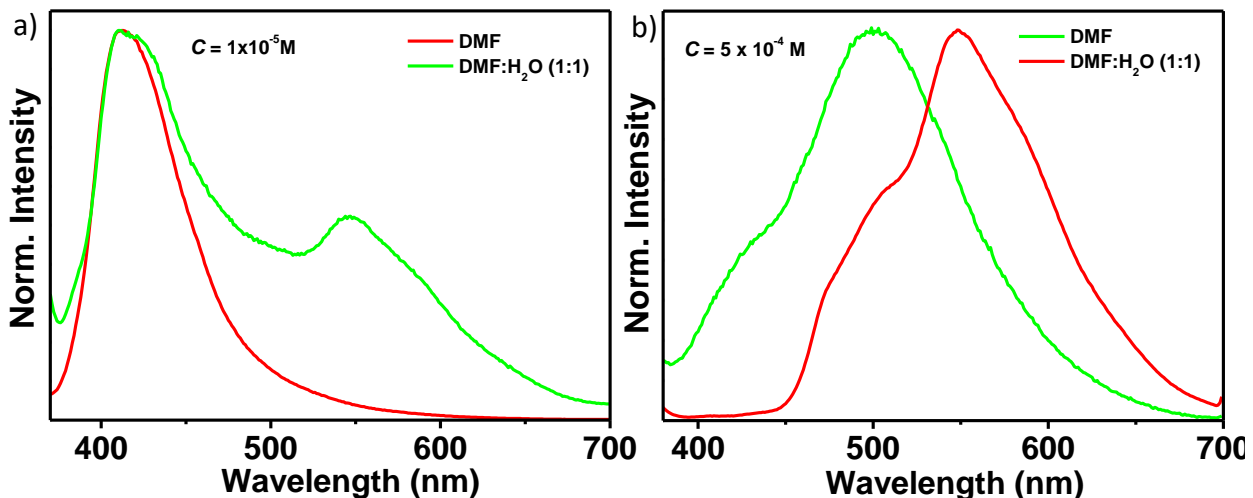


Figure S4. Comparison of the normalized steady state emission of **AqC6** in DMF and DMF:H₂O (1:1) at two different concentrations a) $1 \times 10^{-5} \text{ M}$ and b) $5 \times 10^{-4} \text{ M}$ at 298 K ($l = 1 \text{ cm}$, $\lambda_{\text{ex}} = 360 \text{ nm}$) at 298 K.

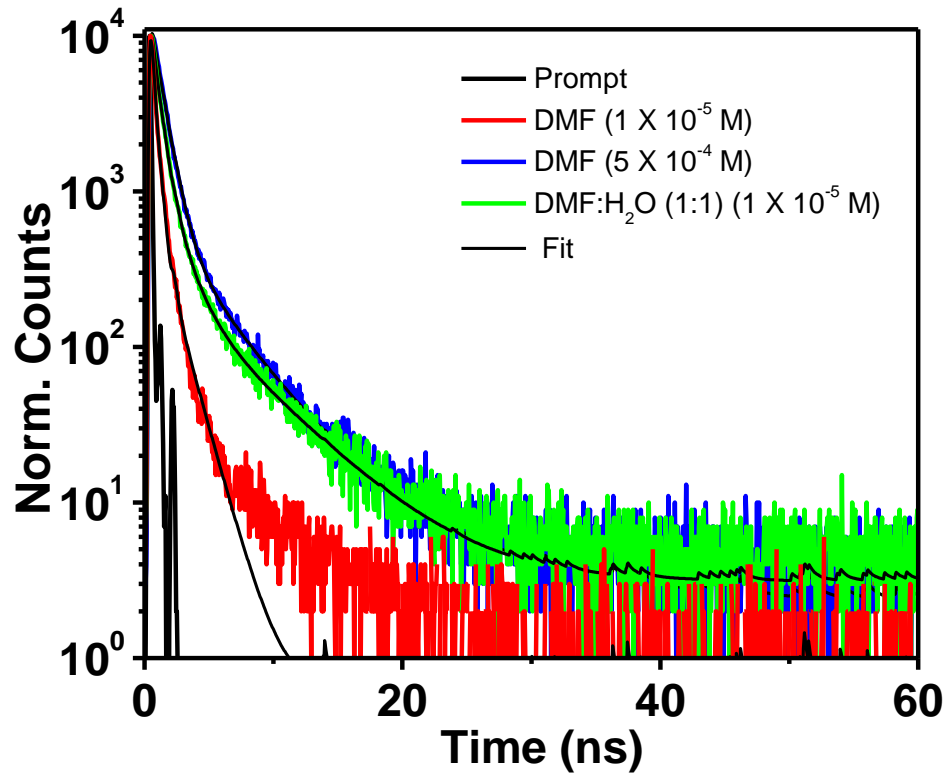


Figure S5. Emission lifetime decay profile of **AqC6** in DMF with increasing concentration ($C = 1 \times 10^{-5}$ M and 5×10^{-4} M, $l = 1$ cm, $\lambda_{\text{ex}} = 374$ nm, $\lambda_{\text{mon}} = 500$ nm) and DMF:H₂O (1:1) ($C = 1 \times 10^{-5}$ M, $l = 1$ cm, $\lambda_{\text{ex}} = 374$ nm, $\lambda_{\text{mon}} = 500$ nm) at 298 K.

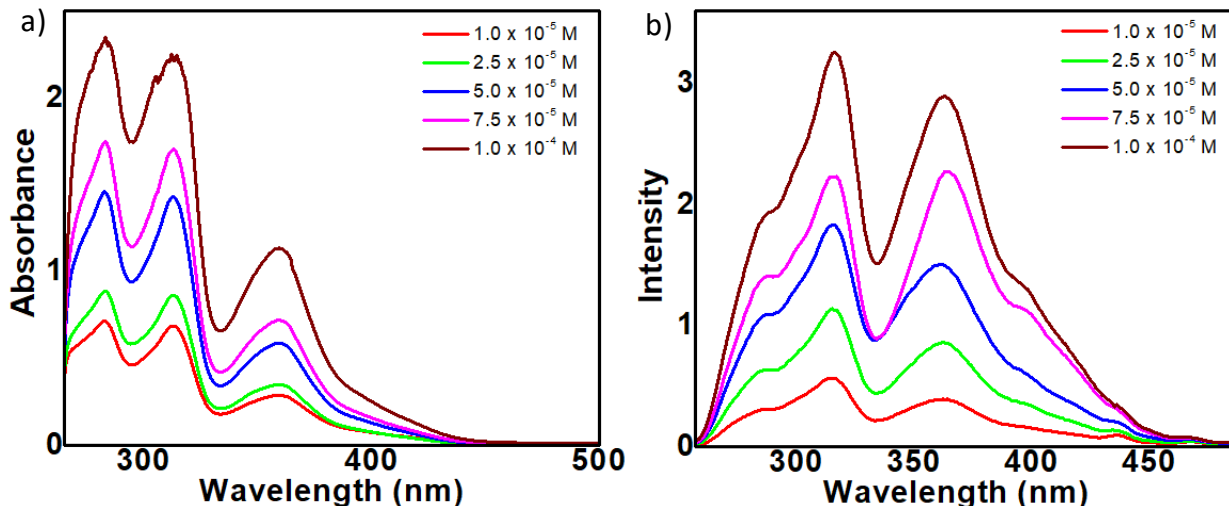


Figure S6. Concentration dependent a) absorption and b) excitation spectra of **AqC6** in DMF at 298 K ($\lambda_{\text{ex}} = 360$ nm).

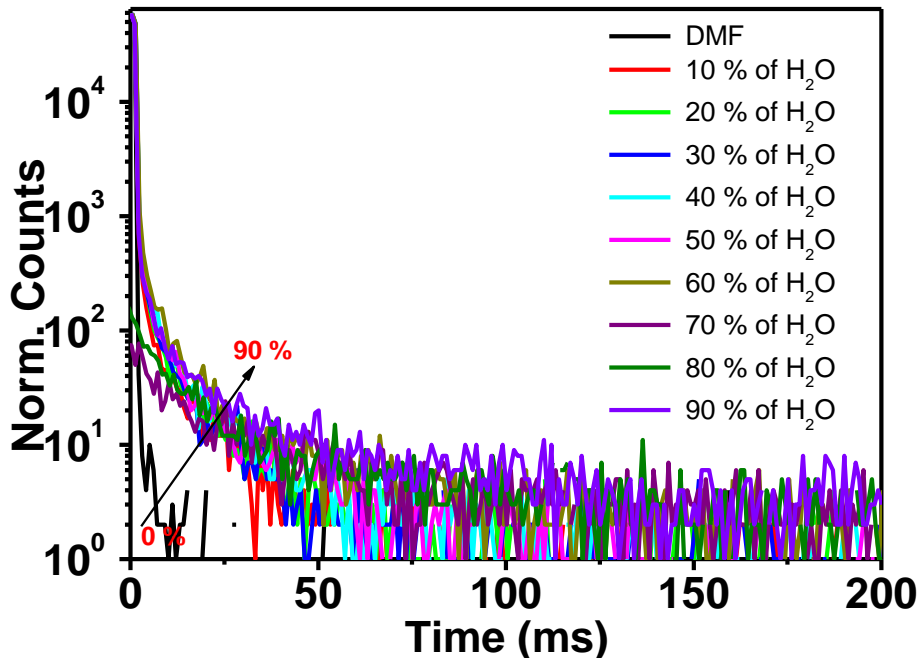


Figure S7. Phosphorescence lifetime decay profile of **AqC6** in DMF and increasing content of H₂O, from 0-90%, recorded at 298 K ($C = 1 \times 10^{-4}$ M, $\lambda_{\text{ex}} = 415$ nm and $\lambda_{\text{mon}} = 560$ nm).

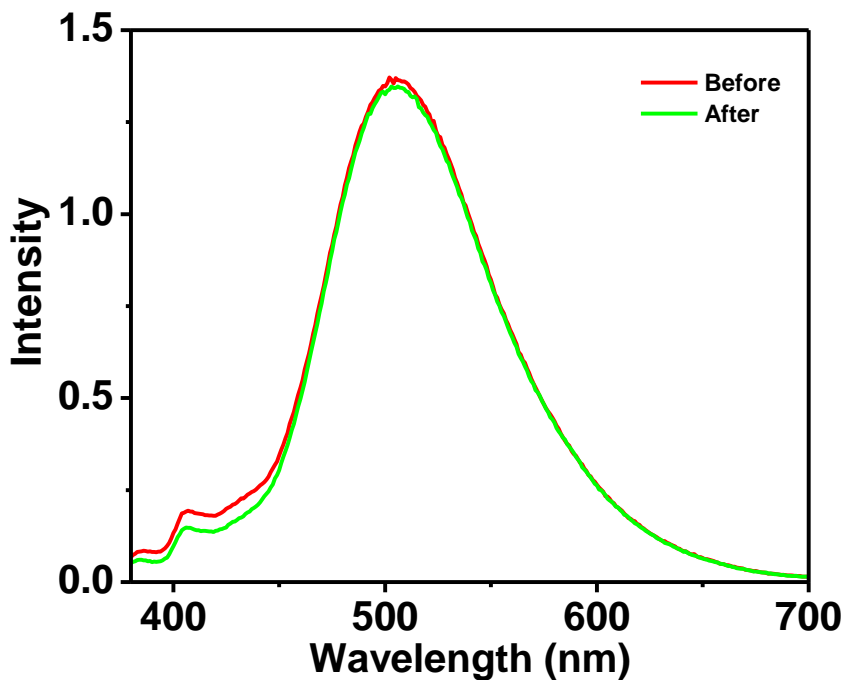


Figure S8. Comparison of the emission spectra of **AqC6** in DMF solution (1×10^{-4} M) before and after purging with oxygen at 298 K.

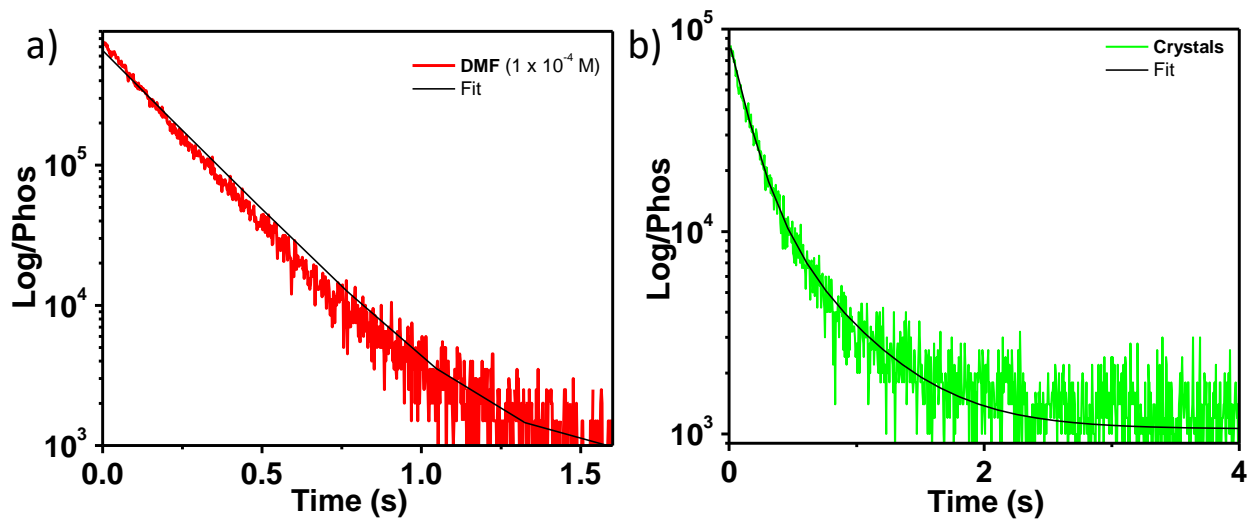


Figure S9. Phosphorescence lifetime decay profile of **AqC6** in a) DMF solution ($C = 1 \times 10^{-4}$ M) and b) crystals at 77 K ($\lambda_{\text{ex}} = 374$ nm, $\lambda_{\text{mon}} = 560$ nm).

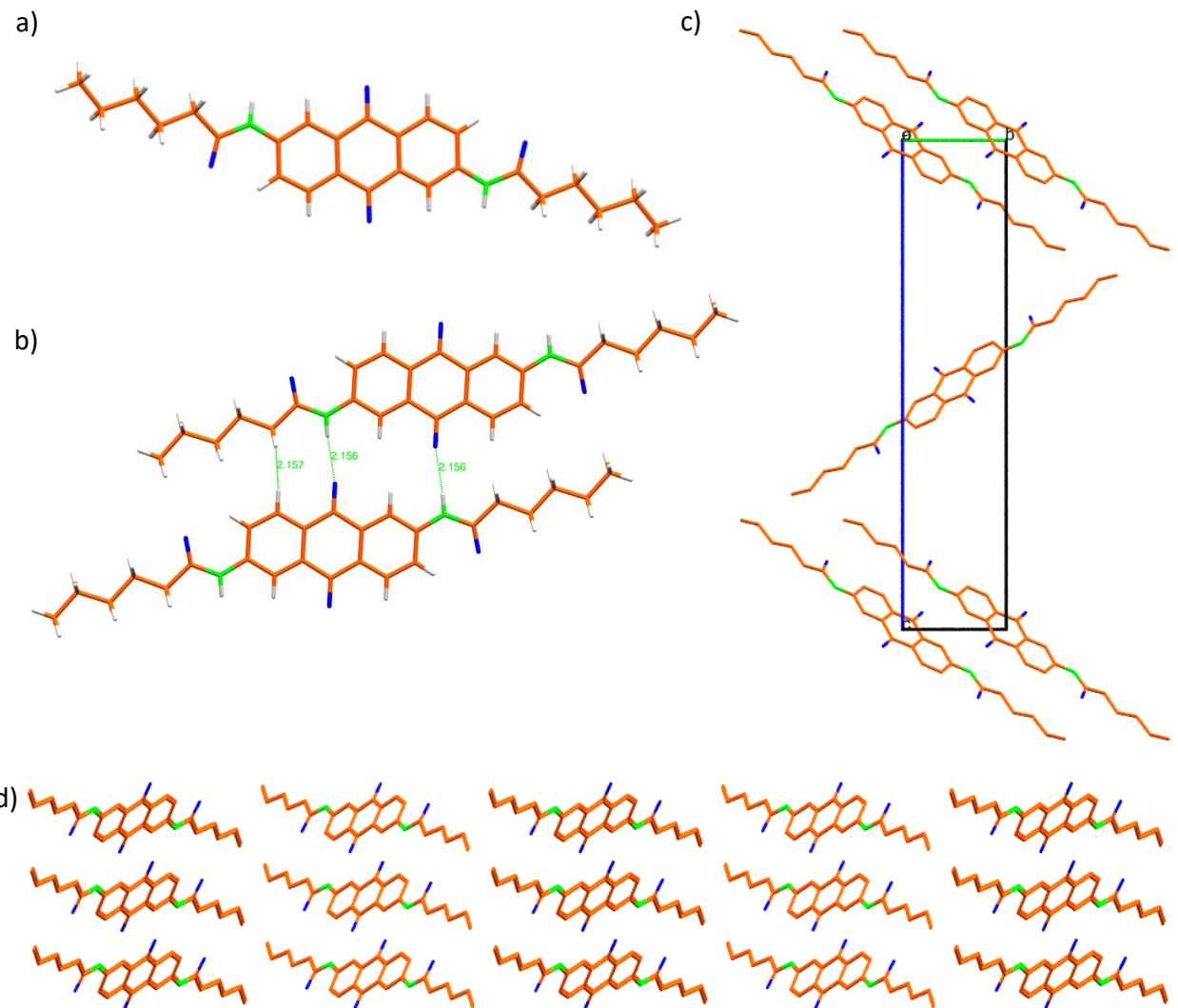


Figure S10. Crystal structure of **AqC6** showing a) single molecule, b) dimer, c) unit cell and d) extended packing along *b* axis, hydrogen is omitted for clarity.

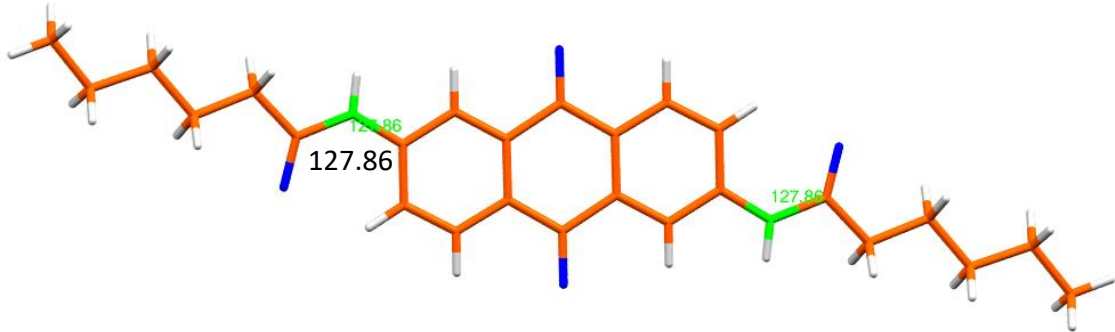


Figure S11. Crystal structure of **AqC6** showing single molecule with bond angle 127.86 ° between anthraquinone and amide planes.

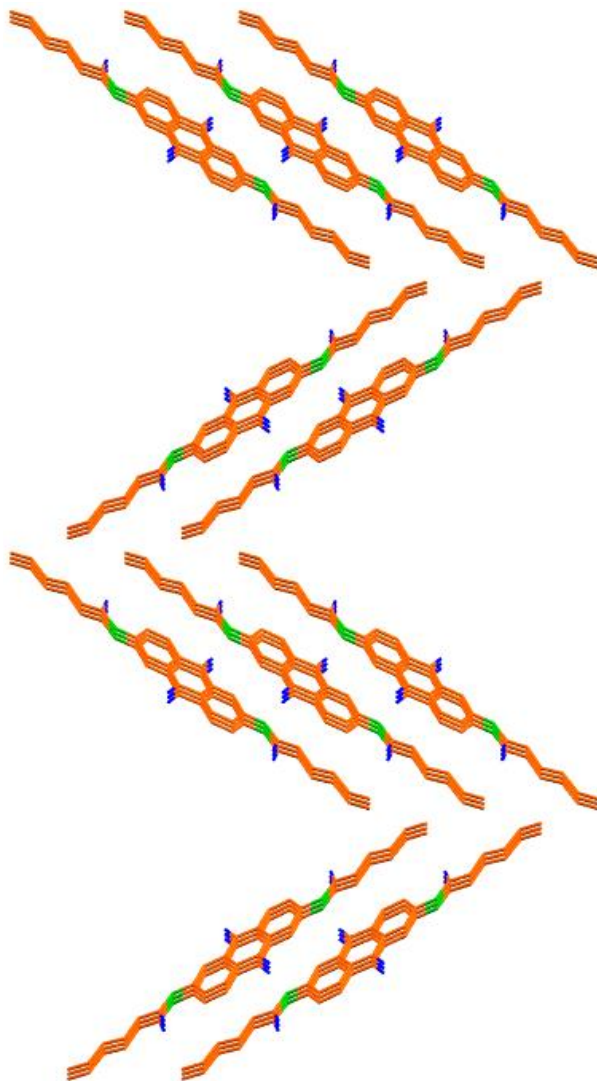


Figure S12. Extended crystal packing of **AqC6** along *a* axis, hydrogen is omitted for clarity.

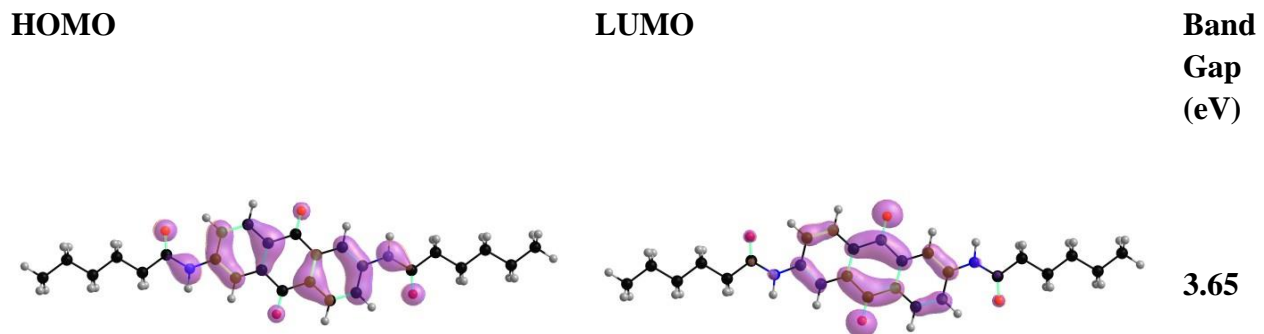


Figure S13. HOMO-LUMO and energy bandgap of **AqC6**.

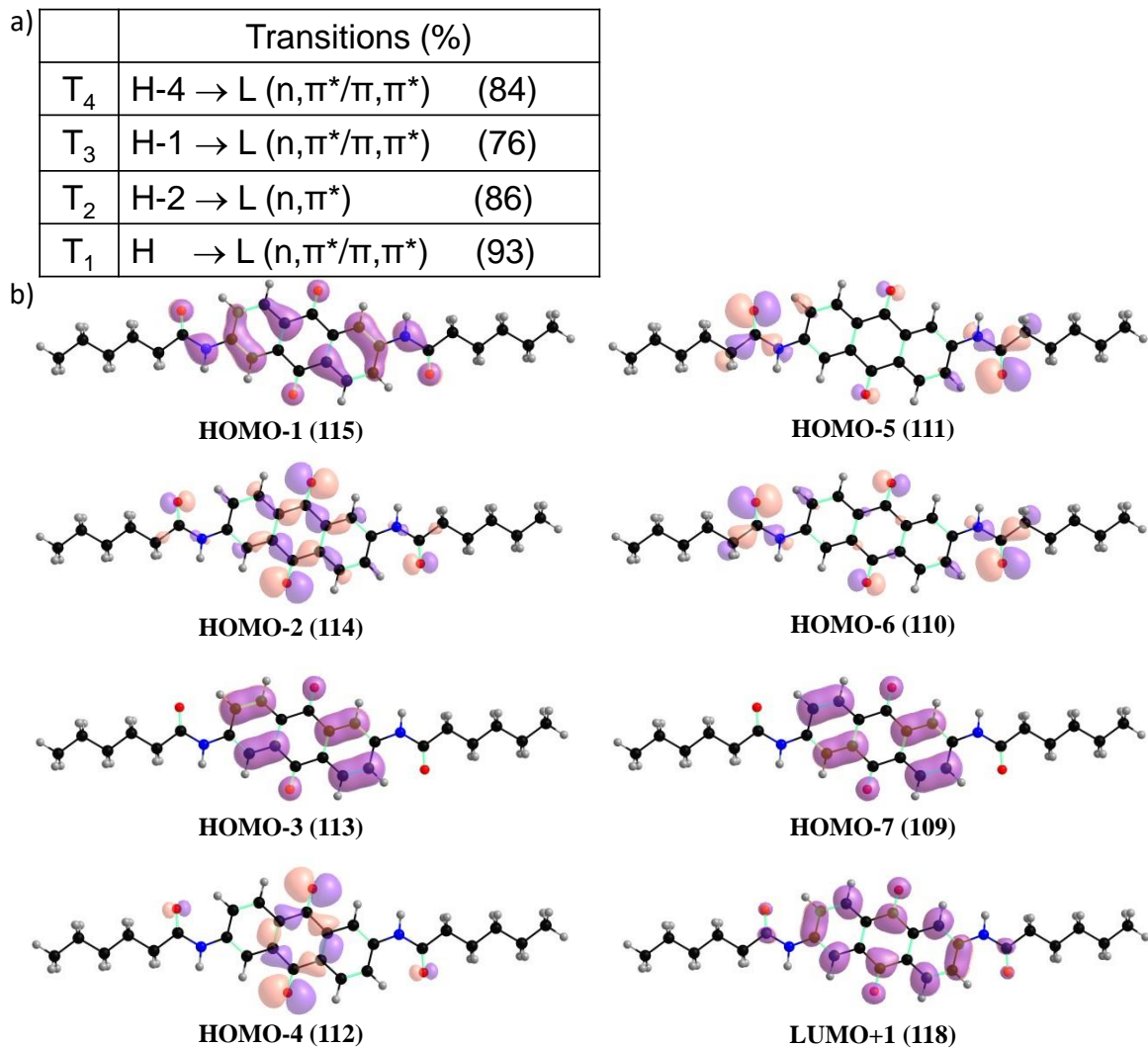


Figure S14. DFT calculations of a) probable electronic transitions and b) involved frontier molecular orbitals.

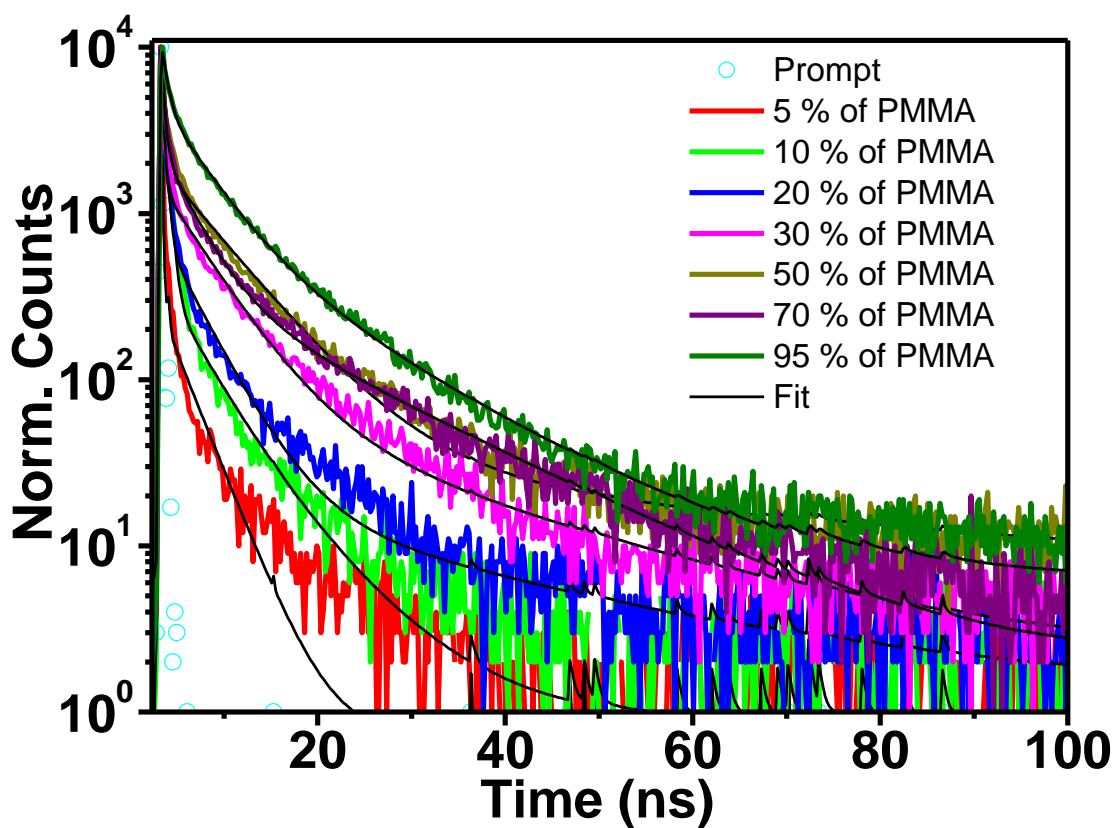


Figure S15. Emission lifetime decay profile of **AqC6** in DMF monitored at 410 nm ($C = 1 \times 10^{-4}$ M, $l = 1$ cm, $\lambda_{\text{ex}} = 374$ nm) with varying amount of PMMA at 298 K.

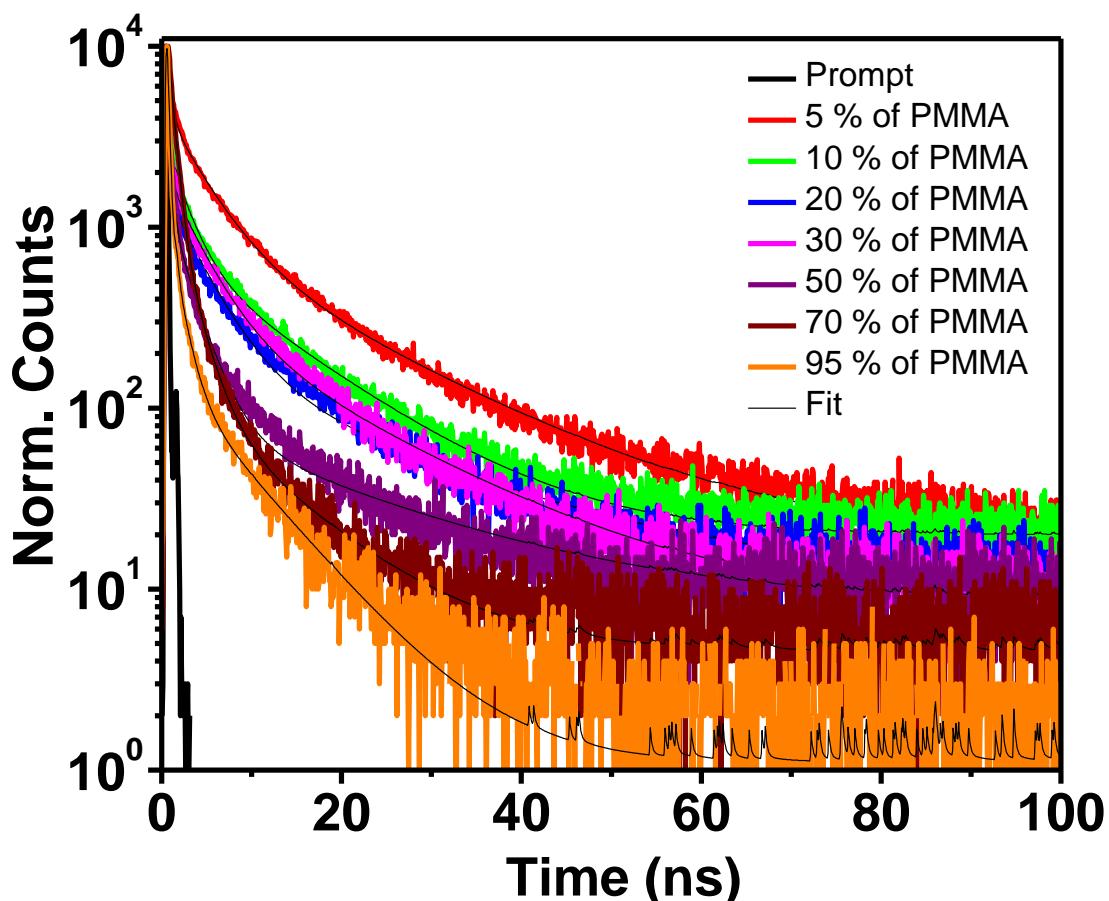


Figure S16. Emission (excimer) lifetime decay profile of **AqC6** monitored at 500 nm ($\lambda_{\text{ex}} = 374$ nm) with varying amount of PMMA at 298 K.

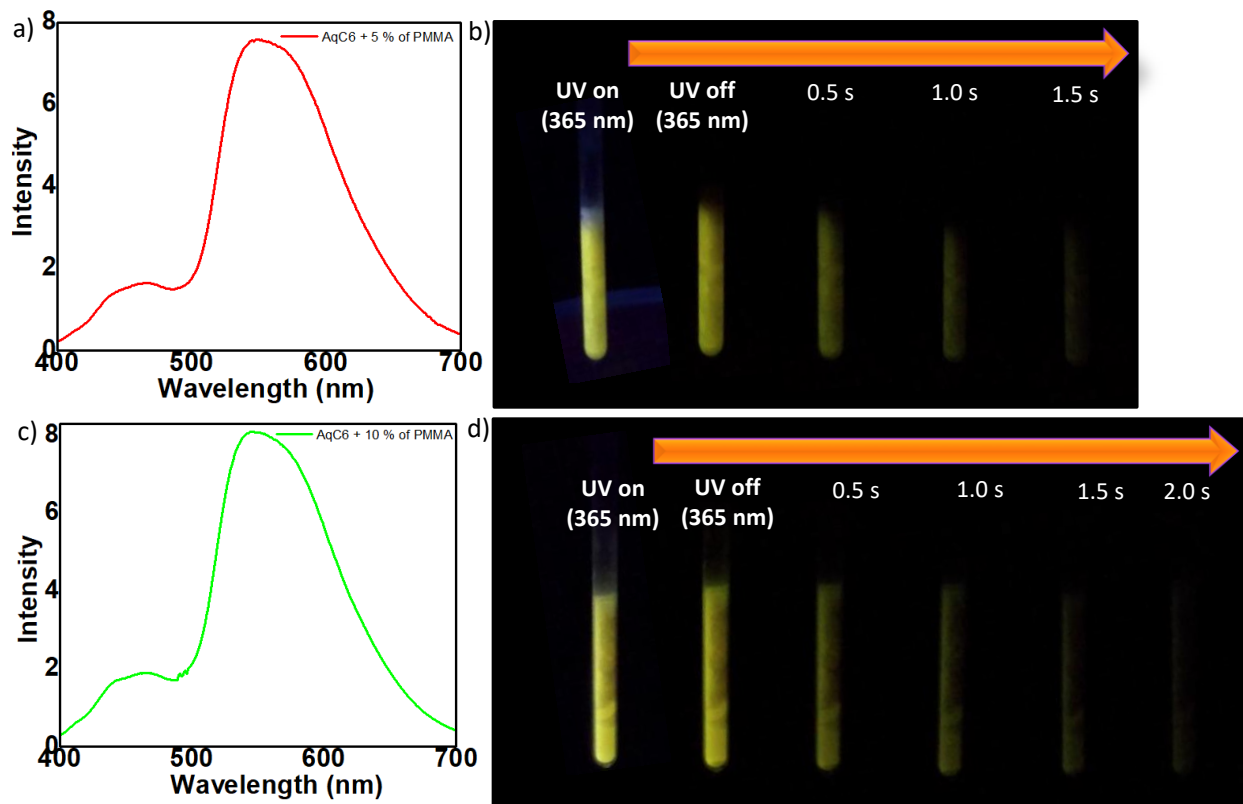


Figure S17. a) Steady-state emission of **AqC6** ($C = 1 \times 10^{-4}$ M) with 5 % of PMMA in DMF at 77 K ($\lambda_{\text{ex}} = 360$ nm) and b) corresponding phosphorescence images of **AqC6** in a quartz tube (3 mm) recorded at different time intervals upon turning off the excitation source (365 nm) after 3 s exposure at 77 K. c) Steady-state emission of **AqC6** ($C = 1 \times 10^{-4}$ M) with 10 % of PMMA in DMF at 77 K ($\lambda_{\text{ex}} = 360$ nm) and d) corresponding phosphorescence images of **AqC6** in a quartz tube (3 mm) recorded at different time intervals upon turning off the excitation source (365 nm) after 3 s exposure at 77 K.

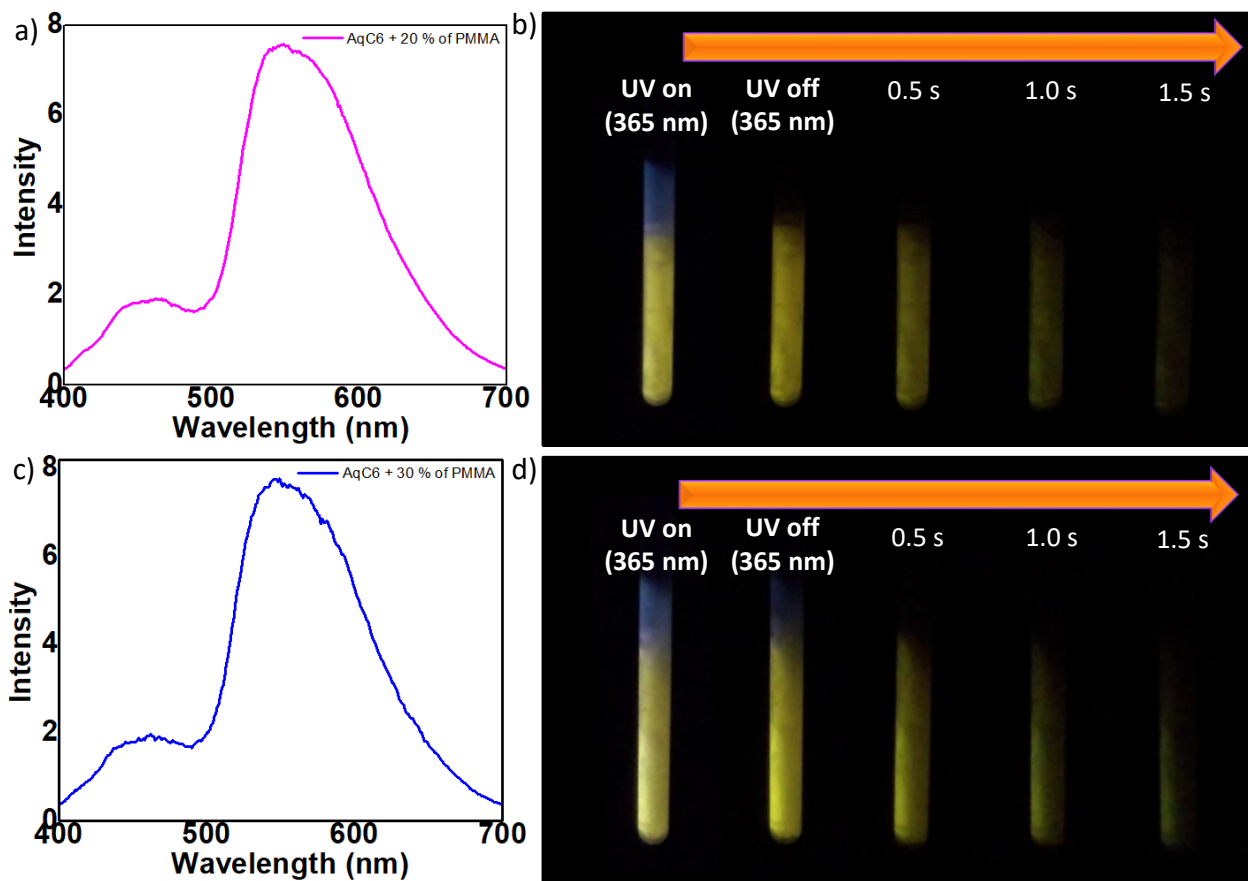


Figure S18. a) Steady-state emission of **AqC6** ($C = 1 \times 10^{-4}$ M) with 20 % of PMMA in DMF at 77 K ($\lambda_{\text{ex}} = 360$ nm) and b) corresponding phosphorescence images of **AqC6** in a quartz tube (3 mm) recorded at different time intervals upon turning off the excitation source (365 nm) after 3 s exposure at 77 K. c) Steady-state emission of **AqC6** ($C = 1 \times 10^{-4}$ M) with 30 % of PMMA in DMF at 77 K ($\lambda_{\text{ex}} = 360$ nm) and d) corresponding phosphorescence images of **AqC6** in a quartz tube (3 mm) recorded at different time intervals upon turning off the excitation source (365 nm) after 3 s exposure at 77 K.

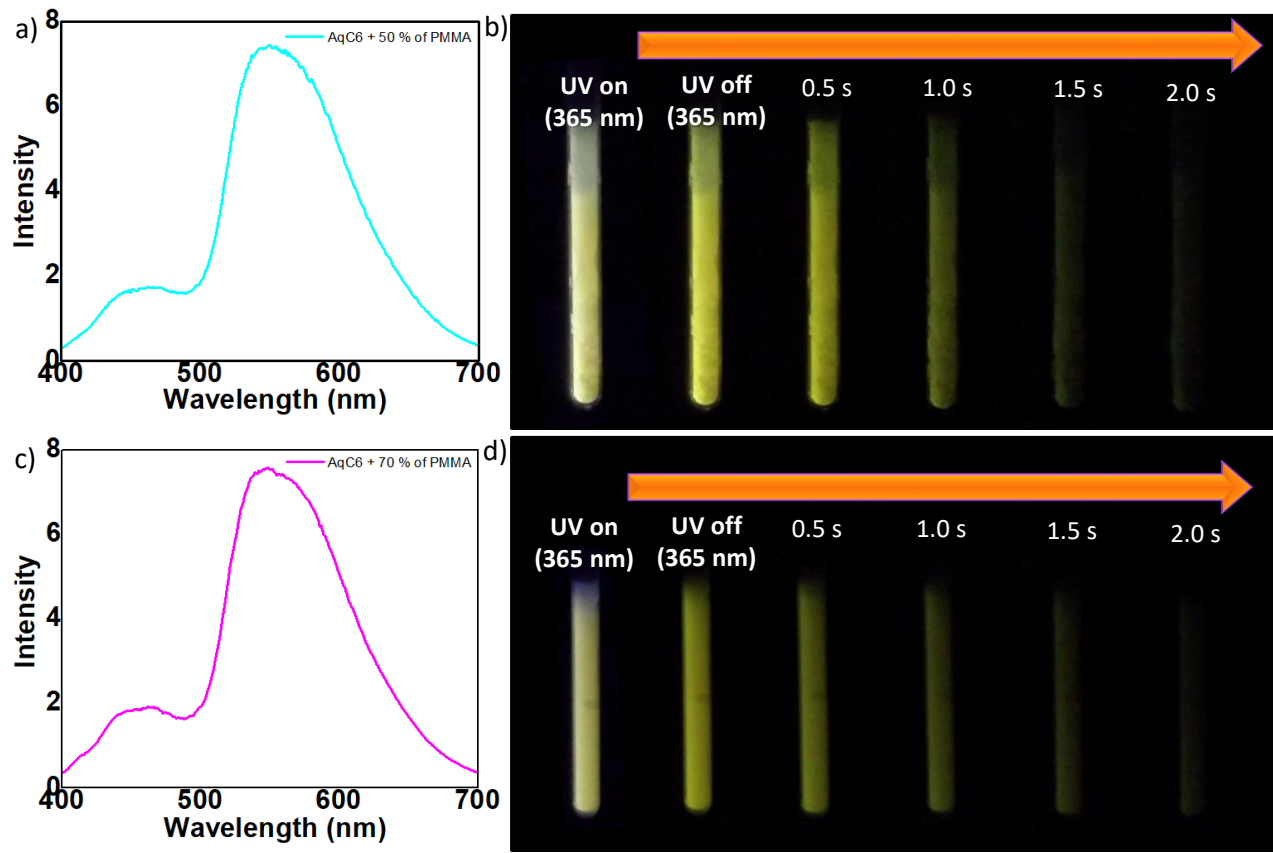


Figure S19. a) Steady-state emission of **AqC6** ($C = 1 \times 10^{-4}$ M) with 50 % of PMMA in DMF at 77 K ($\lambda_{\text{ex}} = 360$ nm) and b) corresponding phosphorescence images of **AqC6** in a quartz tube (3 mm) recorded at different time intervals upon turning off the excitation source (365 nm) after 3 s exposure at 77 K. c) Steady-state emission of **AqC6** ($C = 1 \times 10^{-4}$ M) with 70 % of PMMA in DMF at 77 K ($\lambda_{\text{ex}} = 360$ nm) and d) corresponding phosphorescence images of **AqC6** in a quartz tube (3 mm) recorded at different time intervals upon turning off the excitation source (365 nm) after 3 s exposure at 77 K.

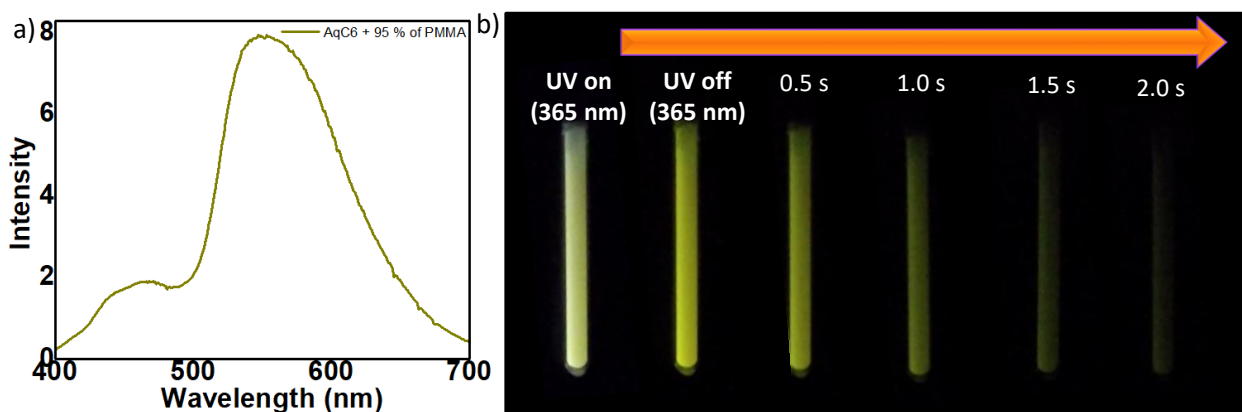


Figure S20. a) Steady-state emission of **AqC6** ($C = 1 \times 10^{-4}$ M) with 95 % of PMMA in DMF at 77 K ($\lambda_{\text{ex}} = 360$ nm) and b) corresponding phosphorescence images of **AqC6** in a quartz tube (3 mm) recorded at different time intervals upon turning off the excitation source (365 nm) after 3 s exposure at 77 K.

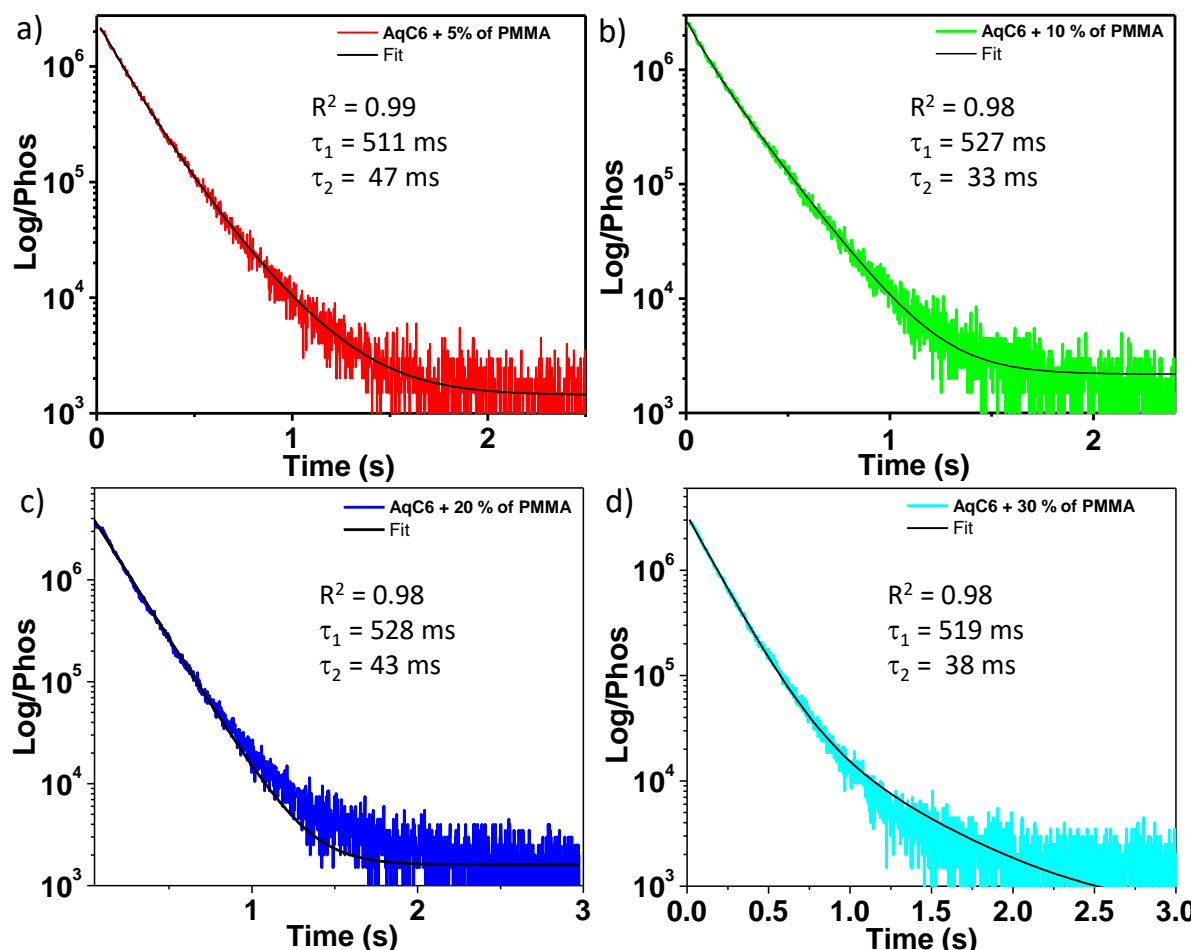


Figure S21. Phosphorescence lifetime decay profile of **AqC6** with a) 5 %, b) 10 %, c) 20 % and d) 30 % of PMMA in DMF at 77 K ($\lambda_{\text{ex}} = 360$ nm).

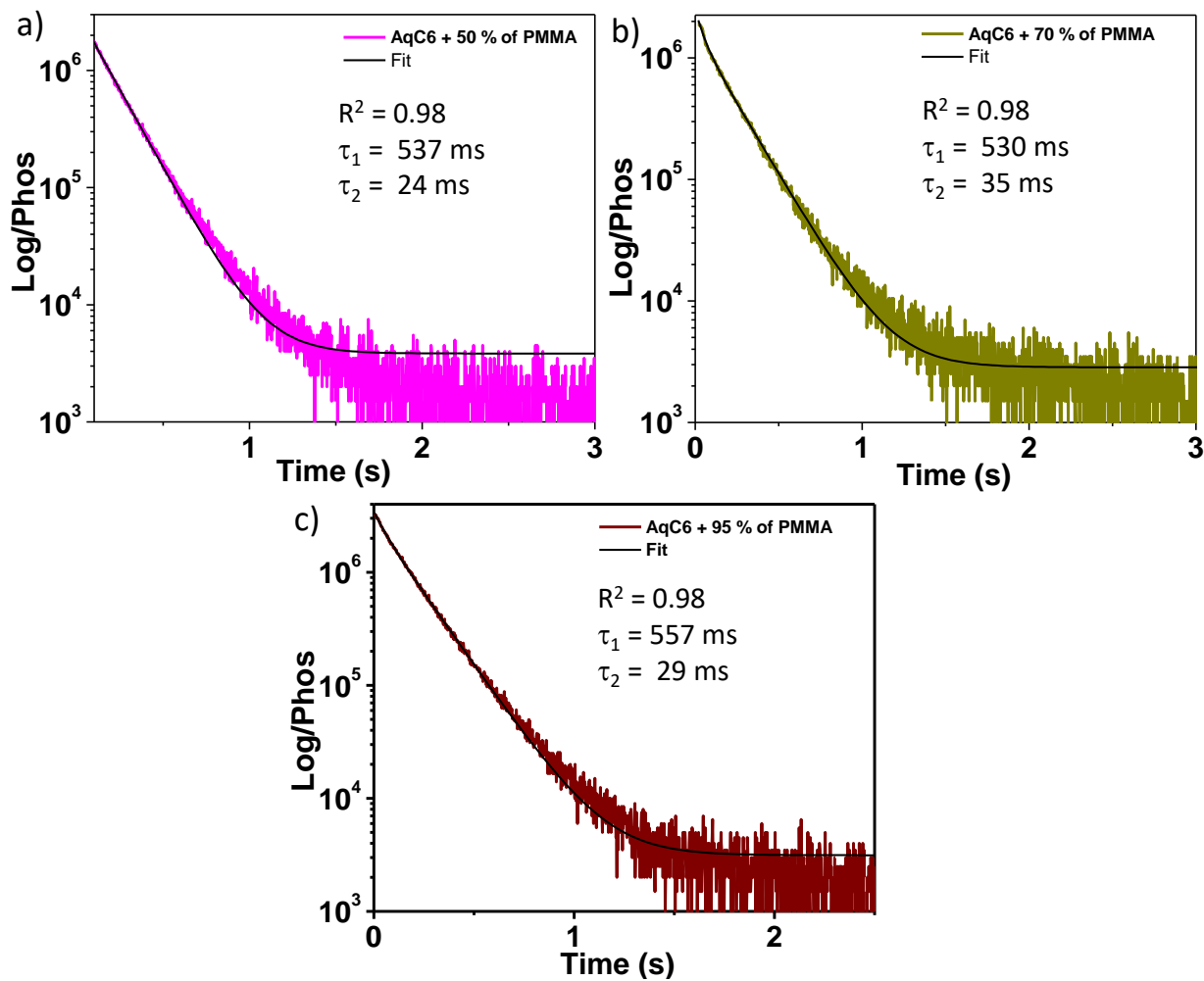


Figure S22. Phosphorescence lifetime decay profile of **AqC6** with a) 50 %, b) 70 % and c) 95 % of PMMA in DMF at 77 K ($\lambda_{\text{ex}} = 360 \text{ nm}$).

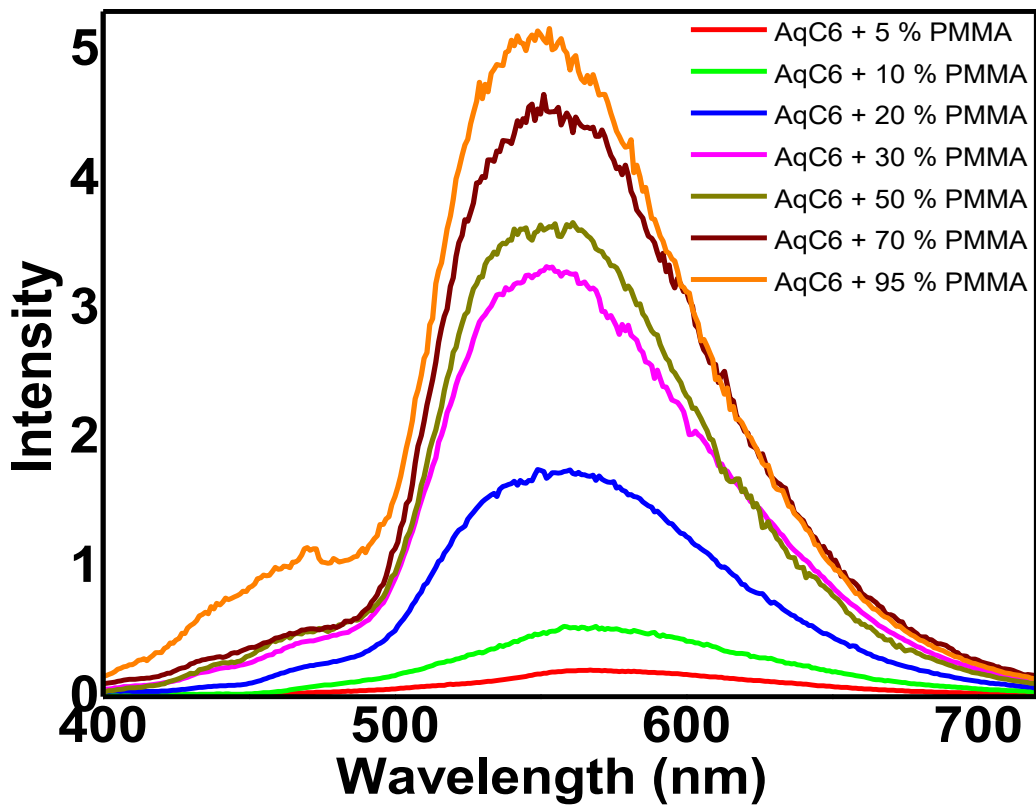


Figure S23. Steady-state emission of **AqC6** thin-films with different percentage of PMMA polymer ($\lambda_{\text{ex}} = 374 \text{ nm}$) at 77 K.

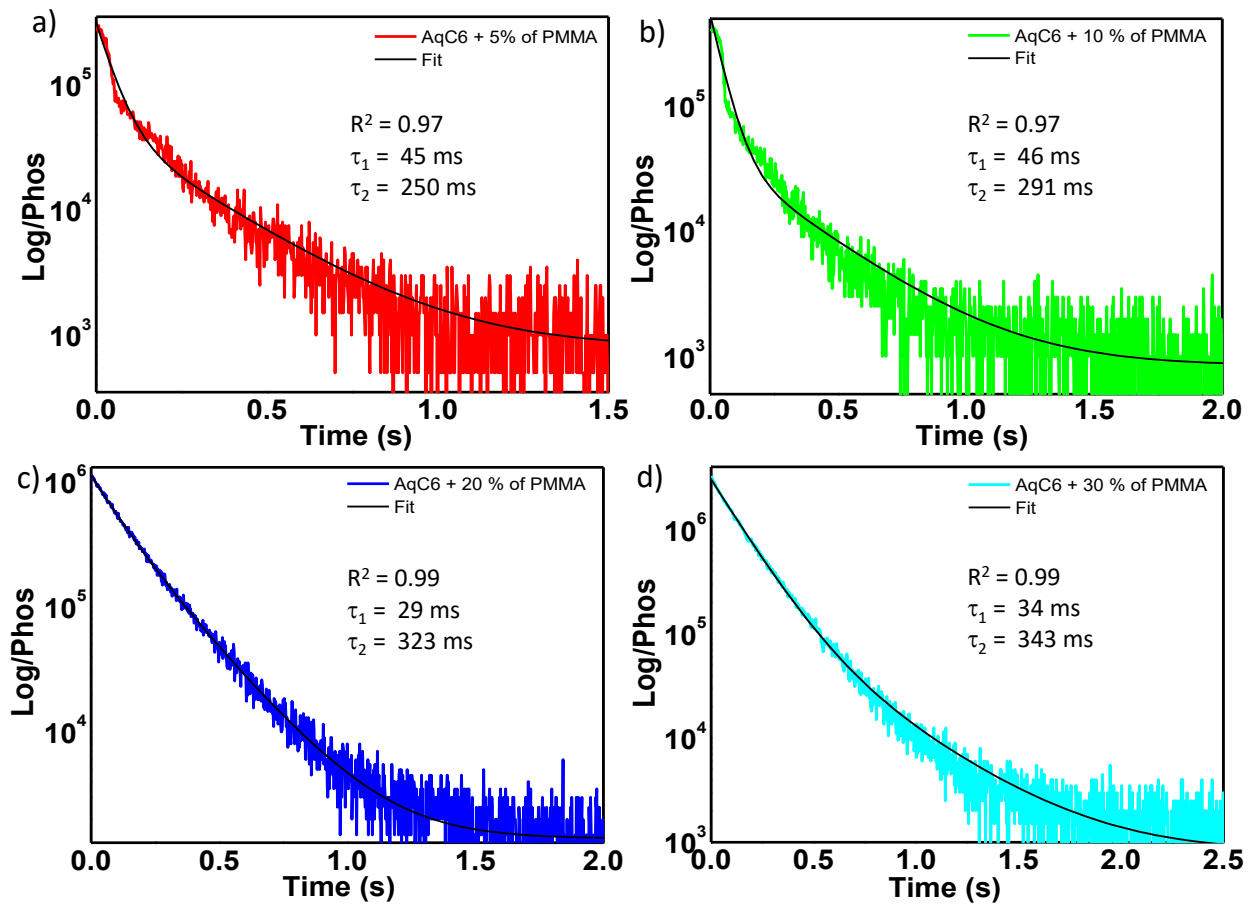


Figure S24. Phosphorescence lifetime decay profile of **AqC6** thin-films with a) 5 %, b) 10 %, c) 20 % and d) 30 % of PMMA at 77 K ($\lambda_{\text{ex}} = 374 \text{ nm}$).

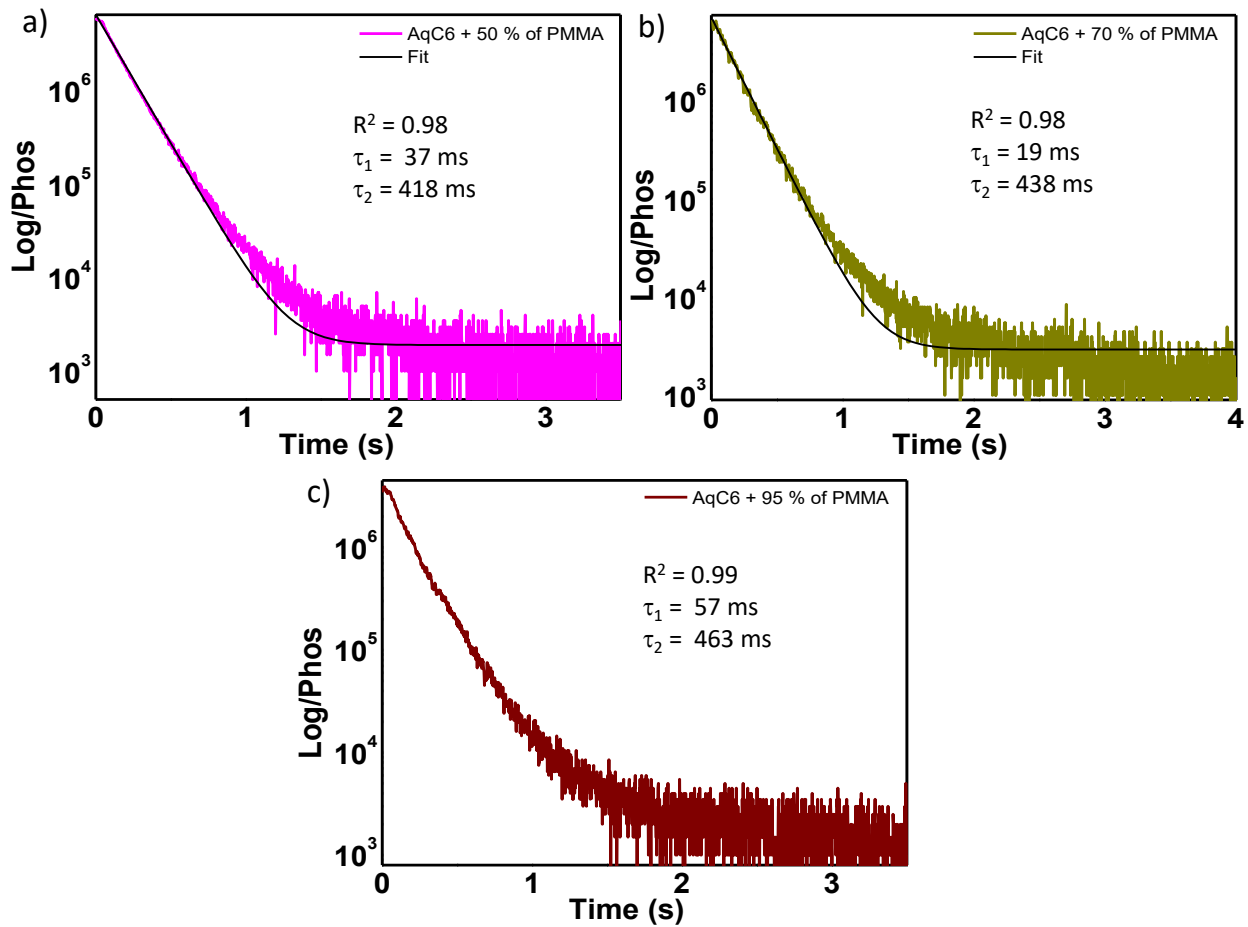


Figure S25. Phosphorescence lifetime decay profile of **AqC6** thin-films with a) 50 %, b) 70 % and c) 95 % of PMMA at 77 K ($\lambda_{\text{ex}} = 374 \text{ nm}$).

Tables

Table S1. Fluorescence lifetime of **AqC6** in DMF ($C = 1 \times 10^{-5}$ M, $\lambda_{\text{ex}} = 374$ nm, $\lambda_{\text{mon}} = 410$ nm) and crystal state ($\lambda_{\text{ex}} = 374$ nm, $\lambda_{\text{mon}} = 560$ nm) at 298 K.

Sample	Fluorescence lifetime (ns)	Contribution (%)
AqC6 in DMF ($\lambda_{\text{mon}} = 410$ nm)	$\tau_1 = 2.9$ $\tau_2 = 0.5$	56 44
AqC6 crystals ($\lambda_{\text{mon}} = 560$ nm)	$\tau_1 = 4.5$ $\tau_2 = 0.8$	89 11

Table S2. Fluorescence QY of **AqC6** in DMF at different concentrations ($\lambda_{\text{ex}} = 360$ nm).

Sample	Concentration	QY (%)
AqC6 in DMF	1×10^{-5} M	0.30
	5×10^{-5} M	0.33
	1×10^{-4} M	0.39

Table S3. Fluorescence lifetime of **AqC6** in DMF with increasing concentration ($C = 1 \times 10^{-5}$ M and 5×10^{-4} M, $\lambda_{\text{ex}} = 374$ nm) and fluorescence lifetime of **AqC6** in DMF:H₂O (1:1) ($C = 1 \times 10^{-5}$ M, $\lambda_{\text{ex}} = 374$ nm) monitored at 500 nm at 298 K.

Sample	Fluorescence lifetime (ns)	Contribution (%)
AqC6 in DMF ($C = 1 \times 10^{-5}$)	$\tau_1 = 1.4$ $\tau_2 = 0.3$	87 13
AqC6 in DMF ($C = 5 \times 10^{-4}$)	$\tau_1 = 26.1$ $\tau_2 = 2.7$ $\tau_3 = 0.8$	69 20 11
AqC6 in DMF:H ₂ O (1:1) ($C = 1 \times 10^{-5}$ M)	$\tau_1 = 31.3$ $\tau_2 = 5.3$ $\tau_3 = 0.5$	64 24 12

Table S4. Phosphorescence lifetime of **AqC6** in DMF at different % of water content ($\lambda_{\text{ex}} = 415$ nm, $\lambda_{\text{mon}} = 560$ nm) at 298 K.

DMF:H ₂ O ratio	Phosphorescence lifetime (ms)	Contribution (%)
100:0	-	-
90:10	$\tau_1 = 0.3$	100
80:20	$\tau_1 = 0.5$ $\tau_2 = 0.1$	53 47
70:30	$\tau_1 = 0.6$ $\tau_2 = 0.1$	62 38
60:40	$\tau_1 = 1.1$ $\tau_2 = 0.1$	76 24
50:50	$\tau_1 = 2.9$ $\tau_2 = 0.1$	70 30
40:60	$\tau_1 = 3.1$ $\tau_2 = 0.6$	62 38
30:70	$\tau_1 = 3.6$ $\tau_2 = 0.3$	62 38
20:80	$\tau_1 = 4.0$ $\tau_2 = 0.3$	52 48
10:90	$\tau_1 = 5.5$ $\tau_2 = 0.4$	54 46

Table S5. Phosphorescence lifetime and related photophysical parameters of **AqC6** crystals ($\lambda_{\text{ex}} = 415$ nm, $\lambda_{\text{mon}} = 560$ nm) at 298 K.

Molecule	Quantum yield (%)	Lifetime (ms)	$K_{\text{nr}}(\text{Phos})$ (s ⁻¹)	$K_{\text{r}}(\text{Phos})$ (s ⁻¹)
AqC6 crystal	4.0	9.0	106.6	0.44

Table S6. Crystal data and structure refinement parameters of **AqC6**.

	AqC6
Molecular formula	C ₂₆ H ₃₀ N ₂ O ₄
Crystal system	Monoclinic
Space group	P2 ₁ /c (14)
a, Å	5.2406 (7)
b, Å	6.5334 (8)
c, Å	31.137 (4)
α, deg	90
β, deg	91.691
γ, deg	90
V, Å³	1065.63
Z, Z'	2, 0

Table S7. π-π* Excitation properties of **AqC6** calculated at the TD-B3LYP/6-31G(d) level.

	ΔE (eV)	λ (nm)	f	Configuration (orbital symmetry)	Coefficient
S0-S1	3.0027	412.91	0.0000	HOMO-2 (114) - LUMO (117)	0.67691
S0-S2	3.0926	400.91	0.0000	HOMO (116) - LUMO (117)	0.69645
S0-S3	3.2687	379.31	0.0000	HOMO-4 (112) - LUMO (117)	0.66870
S0-S4	3.4768	356.60	0.2733	HOMO-1 (115) - LUMO (117)	0.66667
S0-S5	3.9162	316.59	0.0000	HOMO-3 (113) - LUMO (117)	0.65646
S0-S6	4.0624	305.20	0.0000	HOMO-6 (110) - LUMO (117)	0.67541
S0-S7	4.0644	305.05	0.0000	HOMO-5 (111) - LUMO(117)	0.68425
S0-S8	4.1457	299.07	0.1485	HOMO-7 (109) - LUMO(117)	0.53715
S0-S9	4.4314	279.79	0.8682	HOMO (116) - LUMO+1 (118)	0.57529
S0-S10	4.4759	494.97	277.00	HOMO-2 (114) - LUMO+1 (118)	0.67545

	ΔE (eV)	λ (nm)	f	Configuration (orbital symmetry)	Coefficient
S0-T1	2.4815	499.63	0.0000	HOMO (116) - LUMO (117)	0.68086
S0-T2	2.5745	481.59	0.0000	HOMO-2 (114) -LUMO (117)	0.65612
S0-T3	2.6036	476.20	0.0000	HOMO-1(115) - LUMO (117)	0.61505
S0-T4	2.8200	439.66	0.0000	HOMO-4(112) - LUMO (117)	0.64819
S0-T5	3.1569	392.74	0.0000	HOMO-3 (113) - LUMO (117)	0.65758
S0-T6	3.2740	378.69	0.0000	HOMO-7 (109) - LUMO (117)	0.53745
S0-T7	3.6334	341.24	0.0000	HOMO (116) - LUMO+1 (118)	0.58676
S0-T8	3.6841	336.54	0.0000	HOMO-1(115) - LUMO+1 (118)	0.57315
S0-T9	3.9697	312.33	0.0000	HOMO-6(110) - LUMO (117)	0.63812
S0-T10	3.9790	311.60	0.0000	HOMO-5(111) - LUMO (117)	0.65439

Optimized Cartesian coordinates of different complexes (S₀ state) at the B3LYP/6-31G(d) level of theory.

Coordinates of Optimized Structure

O	0.649245794	-2.630304631	-0.000268993
O	6.334086885	1.638641458	-0.000128157
N	5.082671116	-0.289720283	-0.001047237
H	5.168447266	-1.298278605	-0.001263200
C	12.613771914	-0.724177001	0.001096430
H	12.629729360	-1.373252268	0.885371832
H	13.539638474	-0.138024240	0.001994858
H	12.630516723	-1.371786712	-0.884236646
C	11.378794772	0.182229251	0.001301050
H	11.407945877	0.843495925	-0.876052629
H	11.407220798	0.842112401	0.879719346
C	10.057789179	-0.597998539	0.000139978
H	10.028999397	-1.260821825	0.878270474
H	10.029680554	-1.259369530	-0.879108559
C	8.821469356	0.309078973	0.000418539
H	8.840151642	0.969699587	0.875596790
H	8.840856082	0.971243631	-0.873572396
C	7.510588406	-0.479812114	-0.000826676
H	7.463175289	-1.140794630	-0.879124042
H	7.462432112	-1.142382707	0.876228358
C	6.274152111	0.419555288	-0.000604666
C	3.763474717	0.187064024	-0.000764593
C	2.735908418	-0.767167277	-0.000591885

H	2.955112860	-1.831817137	-0.000616229
C	1.400157777	-0.378135658	-0.000382579
C	0.346700828	-1.440104865	-0.000222168
C	1.066010253	0.990974735	-0.000315428
C	3.433877525	1.557557391	-0.000715318
H	4.225625042	2.293069327	-0.000808496
C	2.097742087	1.937912280	-0.000478879
H	1.828706612	2.989282681	-0.000426557
O	-0.649248588	2.630350670	-0.000007061
O	-6.334046350	-1.638630467	-0.000195730
N	-5.082674747	0.289753842	0.000772330
H	-5.168464343	1.298311012	0.001049449
C	-12.613786890	0.724053693	0.000010112
H	-12.630007972	1.372876065	-0.884446084
H	-13.539640643	0.137880290	-0.000459202
H	-12.630296162	1.371915884	0.885162907
C	-11.378789586	-0.182325328	-0.000283075
H	-11.407687533	-0.843350401	0.877261259
H	-11.407439454	-0.842451096	-0.878511424
C	-10.057801350	0.597932513	0.000302409
H	-10.029245729	1.260484983	-0.878040324
H	-10.029487828	1.259575412	0.879339465
C	-8.821462107	-0.309118540	-0.000001299
H	-8.840365376	-0.970054829	-0.874934102
H	-8.840599696	-0.970968236	0.874236000
C	-7.510597349	0.479799485	0.000591946
H	-7.462944303	1.141114041	0.878624102
H	-7.462707443	1.142039308	-0.876729579
C	-6.274142056	-0.419542885	0.000302257
C	-3.763475834	-0.187019849	0.000448246
C	-2.735911112	0.767213151	0.000295715
H	-2.955116389	1.831862858	0.000350949
C	-1.400160407	0.378181778	0.000077138
C	-0.346703361	1.440151004	-0.000076625
C	-1.066012820	-0.990928813	-0.000004742
C	-3.433879393	-1.557512427	0.000368422
H	-4.225627873	-2.293023722	0.000453400
C	-2.097744183	-1.937867126	0.000135055
H	-1.828708501	-2.989237479	0.000077985

Table S8. Thin-film fluorescence lifetime (excimer) of **AqC6** ($\lambda_{\text{ex}} = 374$ nm, $\lambda_{\text{mon}} = 500$ nm) with different percentage of PMMA at 298 K.

AqC6:PMMA ratio (%)	Fluorescence lifetime (ns)	Contribution (%)
5:95	$\tau_1 = 31.8$ $\tau_2 = 2.9$ $\tau_3 = 0.2$	64 23 13
10:90	$\tau_1 = 25.9$ $\tau_2 = 1.6$ $\tau_3 = 0.1$	58 28 14
20:80	$\tau_1 = 20.3$ $\tau_2 = 2.8$ $\tau_3 = 0.1$	57 31 12
30:70	$\tau_1 = 17.1$ $\tau_2 = 2.5$ $\tau_3 = 0.1$	53 29 18
50:50	$\tau_1 = 14.0$ $\tau_2 = 1.7$ $\tau_3 = 0.2$	47 35 18
70:30	$\tau_1 = 7.2$ $\tau_2 = 1.5$ $\tau_3 = 0.4$	44 41 15
95:5	$\tau_1 = 2.9$ $\tau_2 = 5.5$ $\tau_3 = 0.1$	61 23 16

Table S9. Thin-film fluorescence lifetime of **AqC6** with different percentage of PMMA polymer ($\lambda_{\text{ex}} = 374$ nm, $\lambda_{\text{mon}} = \textcolor{red}{560}$ nm) at 298 K.

AqC6:PMMA ratio (%)	Fluorescence lifetime (ns)	Contribution (%)
95:5	$\tau_1 = 0.5$ $\tau_2 = 3.0$	62 38
90:10	$\tau_1 = 0.4$ $\tau_2 = 3.9$ $\tau_3 = 7.9$	6 14 80
80:20	$\tau_1 = 0.5$ $\tau_2 = 4.4$ $\tau_3 = 13.1$	16 23 61
70:30	$\tau_1 = 0.3$ $\tau_2 = 3.2$ $\tau_3 = 16.0$	2 29 69
50:50	$\tau_1 = 0.2$ $\tau_2 = 4.7$ $\tau_3 = 21.9$	2 30 68
30:70	$\tau_1 = 0.3$ $\tau_2 = 3.8$ $\tau_3 = 25.4$	5 30 65
5:95	$\tau_1 = 0.4$ $\tau_2 = 6.6$ $\tau_3 = 39.1$	7 31 62

Table S10. Summary of the fluorescence and phosphorescence of molecule **AqC6** with PMMA at 298 K.

AqC6:PMMA ratio (%)	$\lambda_{\text{max, fluo}}$ (nm)	$\lambda_{\text{max, phos}}$ (nm)	τ_{phos} (ms)	Contribution (%)	ϕ_{phos} (%)	$K_{\text{nr}}(\text{Phos})$ (s^{-1})	$K_r(\text{Phos})$ (s^{-1})
95:5	560	560	$\tau_1 = 106.1$	62	3.7	9.05	0.41
			$\tau_2 = 31.7$	38			
90:10	560	560	$\tau_1 = 126.4$	88	3.9	7.6	0.31
			$\tau_2 = 11.0$	12			
80:20	560	560	$\tau_1 = 161.7$	69	4.2	5.9	0.25
			$\tau_2 = 43.6$	29			
			$\tau_3 = 10.3$	2			
70:30	560	560	$\tau_1 = 168.4$	66	4.6	5.6	0.27
			$\tau_2 = 50.7$	31			
			$\tau_3 = 14.4$	3			
50:50	560	560	$\tau_1 = 174.2$	68	5.1	5.4	0.29
			$\tau_2 = 56.5$	31			
			$\tau_3 = 18.2$	1			
30:70	560	560	$\tau_1 = 171.8$	67	5.7	5.4	0.33
			$\tau_2 = 53.9$	31			
			$\tau_3 = 16.0$	2			
5:95	560	560	$\tau_1 = 164.2$	69	5.5	5.7	0.33
			$\tau_2 = 48.8$	29			
			$\tau_3 = 13.8$	2			

Red marked phosphorescence lifetime is used for the $K_{\text{nr}}(\text{phos})$ and $K_r(\text{phos})$ calculation

References

- S1. J. P. Stephens, J. J. Pan, F. J. Devlin, J. R. Cheeseman, *J. Natural Prod.* **2008**, *71*, 285.
- S2. J. Tirado-Rives, W. L. Jorgensen, *J. Chem. Theory and Comput.* **2008**, *4*, 297.
- S3. M. J. Frisch, G. W. Trucks, H. B. Schlegel, G. E. Scuseria, M. A. Robb, J. R. Cheeseman, G. Scalmani, V. Barone, B. Mennucci, G. A. Petersson, H. Nakatsuji, M. Caricato, X. Li, H. P. Hratchian, A. F. Izmaylov, J. Bloino, G. Zheng, J. L. Sonnenberg, M. Hada, M. Ehara, K. Toyota, R. Fukuda, J. Hasegawa, M. Ishida, T. Nakajima, Y. Honda, O. Kitao, H. Nakai, T. Vreven, J. A. Montgomery, Jr., J. E. Peralta, F. Ogliaro, M. Bearpark, J. J. Heyd, E. Brothers, K. N. Kudin, V. N. Staroverov, R. Kobayashi, J. Normand, K. Raghavachari, A. Rendell, J. C. Burant, S. S. Iyengar, J. Tomasi, M. Cossi, S27 N. Rega, J. M. Millam, M. Klene, J. E. Knox, J. B. Cross, V. Bakken, C. Adamo, J. Jaramillo, R. Gomperts, R. E. Stratmann, O. Yazyev, A. J. Austin, R. Cammi, C. Pomelli, J. W. Ochterski, R. L. Martin, K. Morokuma, V. G. Zakrzewski, G. A. Voth, P. Salvador, J. J. Dannenberg, S. Dapprich, A. D. Daniels, O. Farkas, J. B. Foresman, J. V. Ortiz, J. Cioslowski, D. J. Fox, Gaussian 09 (Revision A.02), Gaussian, Inc., Wallingford CT, **2009**.
- S4. M. Louis, H. Thomas, M. Gmelch, A. Haft, F. Fries and S. Reineke, *Adv. Mater.* **2019**, *31*, 1807887.
- S5. R. Kantam, R. Holland, B. P. Khanna, K. D. Revell, *Tetrahedron Lett.* **2011**, *52*, 5083.